RSC Advances

PAPER

View Article Online
View Journal | View Issue

Cite this: *RSC Adv.*, 2020, **10**, 41065

Biodiesel production from rapeseed oil and low free fatty acid waste cooking oil using a cesium modified natural phosphate catalyst†

Boutaina Rezki,[a] Younes Essamlali,[b] Mina Aadil,[a] Nawal Semlal[c] and Mohamed Zahouily *[ab]

Received 8th September 2020
Accepted 28th October 2020

DOI: 10.1039/d0ra07711a

rsc.li/rsc-advances

The present study focuses on the catalytic activity of cesium modified natural phosphate in biodiesel production from rapeseed oil and low free fatty acids (FFA) used in cooking oil. The catalyst was prepared by impregnation of cesium chloride (CsCl) on the natural phosphate followed by calcination up to 800 °C. The phosphate based catalyst was thermally, structurally, morphologically, and texturally characterized in order to determinate the relationship between its physicochemical properties and its catalytic activity. The chosen catalyst was demonstrated to be an active catalyst for the transesterification of rapeseed oil achieving a biodiesel yield of 99.55% under suitable reaction conditions: a methanol to oil molar ratio of 12 : 1, reaction temperature of 70 °C, catalyst amount of 4 wt% based on oil weight and reaction time of 6 h. Results from low FFA waste cooking oil transesterification indicated that a methyl esters yield of 99.52% could be obtained. Furthermore, results from esterification/transesterification of acidified rapeseed oil indicate that a yield of 93% may be obtained, thus giving rise to a potential application in 2nd generation biodiesel production from low acidic oils. Some important physicochemical properties of the obtained biodiesel were evaluated and compared with the EN14214 and ASTM D-6751 standards for biodiesel specifications.

Introduction

Petroleum consumption has been increasing exponentially over recent decades due to the ever increasing population and the steady growth in transportation and the industrialization sector.[1] This huge consumption of petroleum brings about serious issues concerning the rapid depletion of fossil fuels and their contribution to climate change in terms of global warming. These issues have triggered research to find an alternative energy source to petroleum-derived fossil fuels. In recent years, biodiesel, or fatty acid methyl ester (FAME), has emerged as an alternative fuel source since it exhibits similar physicochemical properties to conventional petroleum-based diesel. Furthermore, biodiesel is even better than petroleum diesel in terms of biodegradability, non-toxicity and reduced NO_x and particulate emission.[2] Conventionally, biodiesel is produced by transesterification of vegetable oils or animal fats, in the presence of homogeneous acid or base catalysts *e.g.* H_2SO_4,[3] KOH, NaOH and CH_3ONa that are highly reactive under mild reaction conditions and give high FAME yields.[4,5] The transesterification reaction occurred in three consecutive steps in which the triglyceride molecule is converted into diglyceride molecule which is converted into monoglyceride which is in turn converted into methyl esters along with glycerol as a by-product.[6] Unfortunately, the homogeneous base catalytic process suffers from several drawbacks such as soap formation, tedious purification processes, production of large amount of wastewater and difficulty to remove the catalyst after the reaction.[7] The problems associated with the use of homogenous catalysts could be avoided by using solid base or acid heterogeneous catalyst, allowing considerably reduced process cost and simplifying biodiesel production steps.[8] During the last few decades, a variety of catalysts such as alkaline-earth metal oxides (CaO, SrO, MgO), alkali-doped metal oxides like Li, K and Na doped CaO and MgO,[9,10] Al_2O_3 modified alkali metals like $NaNO_3/Al_2O_3$, $LiNO_3/Al_2O_3$ (ref. 9) KF/Al_2O_3,[11] mixed metal oxides Al_2O_3/MgO,[12] CaO/Al_2O_3,[13] CaO–MgO/Al_2O_3,[14] zeolites[15] as well as hydrotalcites have been synthesized and their catalytic activity was investigated in biodiesel production from edible or non-edible oil. In addition to these catalytic systems, cesium doped CaO such as CsF/CaO,[16] cesium modified silica catalyst,[17] CsF/Al_2O_3 (ref. 18) were also reported to promote efficiently the transesterification reaction to produce biodiesel.

[a]*Laboratoire de Matériaux, Catalyse & Valorisation des Ressources Naturelles, URAC 24, Faculté des Sciences et Techniques, Université Hassan II, Casablanca B.P. 146, 20650, Morocco. E-mail: mohamed.zahouily@fstm.ac.ma*

[b]*MAScIR Foundation, VARENA Center, Rabat Design, Rue Mohamed El Jazouli, Madinat Al Irfane, Rabat, 10100, Morocco. E-mail: m.zahouily@mascir.com*

[c]*Innovation Team, OCP S.A., El Jadida, BP 118, Morocco*

† Electronic supplementary information (ESI) available: FTIR, ^{1}H-NMR and GC analysis. See DOI: 10.1039/d0ra07711a

Recently, many researchers have focused on the use of catalysts derived from solid waste or natural resources such as coral, mollusk, eggshells and animal bone to produce biodiesel. Particularly, natural hydroxyapatite based-materials derived from fish, chicken, bovine and sheep bones have been extensively studied as heterogeneous catalysts for biodiesel production due to their low solubility in biodiesel and methanol, ion-exchange ability and acid–base adjustability.[19–21] These studies revealed that the impregnation of alkaline active component into calcium phosphate based catalyst might be helpful for transesterification process.[22] The use of such catalysts provides the benefit of being cost-effective which can reduce the overall cost of biodiesel production. Apatite type structure such as sodium modified synthetic hydroxyapatite and fluoroapatite and potassium doped calcined pig bones have been widely studied for biodiesel production from various vegetable oils and waste cooking oil, allowing obtaining high fatty acid methyl esters yields.[23,24]

Morocco has various sedimentary phosphate deposits containing mineral apatites having a chemical structure similar to that of carbonate-fluoroapatite commonly called francolite ($Ca_{10-a}M_a(PO_4)_{6-b-c}(CO_3)_bY_cF_2X_{2-d}$) with various isomorphic substitutions.[25,26] Phosphate rocks are complex raw materials and contains the apatite groups in association with a wide assortment of accessory minerals, mainly fluorides, carbonates, clays, quartz, silicate, and metal oxides.[27] It is a readily available, cheap, nontoxic and a non-pollutant material.[28] The natural phosphate (NP) has been widely studied as efficient catalysts for various organic transformations, for example, in Michael-addition,[29] Knovenagel condensation,[26] Claisen–Schmidt condensation,[30,31] Friedel–Crafts alkylation,[32] Suzuki–Miyaura coupling reaction[32] and transesterification reaction.[25] The physicochemical properties of NP particularly its ion exchange ability like other apatite structures allow the design of various NP-based catalysts and make them an appropriate candidate for biodiesel production. Hence, to increase the basic strength of the NP, first group elements in the periodic table are considered as the best choice to generate efficient base and active component; cesium (Cs) is one of the attractive due to high value of alkalinity. Therefore, the present work focuses on the study of the catalytic activity of cesium modified natural phosphate in biodiesel production from rapeseed oil and low free fatty acid used cooking oil. The catalyst was prepared by the conventional incipient-wetness impregnation of CsCl into NP followed by calcination at 800 °C, then it was thermally, structurally, texturally, and morphologically characterized in order to highlight the relationship between its physicochemical properties and its catalytic activity. The effect of reaction parameters such as reaction temperature, catalyst amount, methanol to oil molar ratio, reaction time and feedstock acidity on the FAME yield were also investigated.

Experimental

Materials and physical experiments

Phosphate samples used in this study come from an extracted ore of Khouribga deposits, an important source of phosphate in Moroccan kingdom. Cesium chloride (CsCl) was purchased from Sigma Aldrich, rapeseed oil was purchased from a local company in Mohammedia city, Morocco and was directly used without further treatment. Waste cooking oil (WCO) was supplied by a local restaurant and was filtered before being used in the transesterification experiment to eliminate solid suspensions. All chemicals were analytical grade and were directly used without any further purification.

Feed stock's characterization

Some important physical and chemical properties of the rapeseed oil and the waste cooking oil (WCO) used as feedstocks for biodiesel production are listed in Table 1. The refined rapeseed oil exhibited very low water content and free fatty acid content.

Catalyst preparation

Natural phosphate was pretreated using the procedure reported in a previous work.[33] The pretreated natural phosphate was calcined at 700 °C for 4 h to eliminate moisture from its surface, and finally grounded (63–125 μm) before being used. The chemical composition of treated NP was determined as: CaO (50.47%), P_2O_5 (30.74%), CO_2 (6.64%), SiO_2 (5.91%), F (3.6%), Al_2O_3 (0.43%), SO_3 (1.83%), Fe_2O_3 (0.2%) and other negligible elements.

The calcined natural phosphate named NP was impregnated with CsCl according to the conventional incipient-wetness impregnation. In a typical synthesis, to prepare 10 wt% CsCl impregnated NP, 0.9 g of CsCl was dissolved in 120 mL double distilled water for 10 minutes until complete dissolution to make an homogeneous cesium chloride solution of 0.0445 M, then 9 g of previously grounded NP was slowly added to cesium precursor solution and the mixture was vigorously stirred under vigorous magnetic stirring at 700 rpm for 2 h. The resultant slurry was then evaporated to dryness at 90 °C and the solid material produced was grounded, sieved through a 125 μm sieve and finally calcined at 800 °C for 4 hours to yield the 10CsCl/NP-800 catalyst. The same procedure was adopted to synthesize 5CsCl/NP-800, 30CsCl/NP-800 and 50CsCl/NP-800.

Table 1 Physical and chemical properties of rapeseed oil and waste cooking oil

		Analysis results	
Properties	Unit	Rapeseed oil	WCO
Molecular weight	$g\ mol^{-1}$	869.16	871.01
Density at 20 °C	$g\ cm^{-3}$	0.918	0.929
Kinematic viscosity at 24 °C	$mm^2\ s^{-1}$	63.286	68.568
Acid number	$mg_{KOH}\ g^{-1}$	0.06	1.06
Moisture content	wt%	0.03	—
Iodine value	$g_{I_2}\ kg^{-1}$	97	—
Flash point	°C	270	—
Peroxide value	meq. O_2 per kg	0.2	—

Catalyst characterization

Thermogravimetric analysis was performed on a TA Instrument Q500 apparatus, all experiments were conducted at a heating rate of 10 °C min^{-1} from a room temperature up to 1000 °C using approximately 15 mg of sample. X-ray diffraction (XRD) data of the prepared catalysts were collected at room temperature using a D2 PHASER diffractometer, with the Bragg–Brentano geometry, using CuKα radiation ($\lambda = 1.5406$ Å) at 30 kV and 10 mA. The patterns were scanned through steps of 0.02 (2θ). Scanning electron microscopy (SEM) analysis was carried out on a Tecnai G2 microscope at 120 kV. Fourier transform infrared (FT-IR) spectra of samples in KBr were recorded using a Bruker Vector 22 spectrometer over the range of 4000–400 cm^{-1} at a resolution of 16 cm^{-1}. Solid state ^{31}P nuclear magnetic resonance experiments were recorded on a Bruker Advance 600 MHz spectrometer. The powder samples were packed into 4 mm zirconia magic-angle spinning (MAS) rotors and spin at a rotation frequency of 10 kHz. Textural characteristics, Brunauer–Emmett–Teller (BET) surface area and average pore diameter were determined by N_2 adsorption–desorption technique using a Micromeritics 3FLEX analyzer. Prior to measurement, all samples were degassed at 250 °C during 8 h under vacuum. The surface area of samples was calculated according to the Brunauer–Emmett–Teller (BET) method using adsorption data whereas the pore size and volume were estimated using the Barrett–Joyner–Halenda (BJH) method. The basic strengths of the catalysts were determined by adsorption of phenol. About 100 mg of the catalyst sample was suspended in 25 mL of phenol in cyclohexane (100 mg L^{-1}) and left to equilibrate for 5 h under stirring. After equilibrium, the catalyst was recovered by centrifugation and the solution was analyzed by UV visible spectrometer at 270 nm against a calibration curve.

Transesterification reaction

Reaction procedure

Transesterification of rapeseed oil. The transesterification reactions were carried out in a 100 mL round-bottom flask equipped with reflux condenser and magnetic stirrer. In typical experiment, the appropriate amount of oil was firstly introduced in the flask, then the quantity of methanol based on the methanol to oil molar ratios (3 : 1 to 16 : 1) and the catalyst with respect to the starting oil weight (2–8 wt%,based on oil weight) were added. The reaction mixture was heated to the desired temperature (40–80 °C) under constant magnetic stirring (800 rpm). Upon the completion of reaction, the mixture was cooled to ambient temperature and the catalyst was recovered by centrifugation at 4500 rpm. Subsequently, the excess of methanol was recovered by rotary evaporation under reduced pressure. Finally, a phase separation in a separating funnel resulted in the isolation of the methyl esters and glycerol. The biodiesel was recovered from the top layer while glycerol from the bottom.

Transesterification of waste cooking oil. Transesterification reaction of WCO was carried out according to the following pre-optimized conditions: typically, 26 g of WCO, 14.5 mL of methanol and 4 wt% catalyst based on the weight of the used WCO were introduced in a round bottom flask reactor and the mixture was allowed to react at 70 °C for six hours under vigorous magnetic stirring. After reaction completion, the catalyst was recovered by simple centrifugation and the crude reaction mixture was subjected to a rotary evaporation to remove the unreacted methanol and finally phase separation resulted in the separation of the methyl esters and glycerol.

The reaction progress was monitored by ^1H-NMR analysis (Bruker Avance 600 MHz) using deuterated chloroform ($CDCl_3$) as a solvent and tetramethylsilane (TMS) as an internal standard. The oils conversions were determined using the calculation methods reported by Gelbard *et al.*[34] and Liza *et al.*[35]

The methyl esters content, triglyceride, diglyceride and monoglyceride contents were also quantified by GC-MS (Agilent 7890A Series GC) equipped with a DB-17HT capillary column (30 m × 250 mm × 0.15 mm). Before injection, 10 mg of the prepared biodiesel and 10 mg of methyl 10-undecaoate were diluted by 1 mL of chloroform. About 1 μL of the diluted sample was injected into the DB-17HT capillary column using helium as the carrier gas at a constant flow rate of 5 mL min^{-1} and split less injection mode. The initial oven temperature was set at 50 °C (held for 1 min) and subsequently increased to 180 °C at a heating rate of 25 °C min^{-1}, and then the oven temperature was further increased to 230 °C at 7 °C min^{-1} rate and held for 0 min. The oven temperature was finally extended to 360 °C at 30 °C min^{-1} and maintained at this temperature for 10 min. The temperatures of ion source and quadruple were maintained at 230 and 150 °C, respectively. FAME identification was performed using NIST 2011 MS Library. The FAME contents were calculated according to the following equation:

$$\text{Ester content } (\%) = (\sum A_{\text{FAME}} - A_{\text{St}}) \times m_{\text{St}}/(A_{\text{St}} \times m) \times 100$$

where $\sum A_{\text{FAME}}$ the sum of the areas under all is peaks from FAMEs; A_{St} is the area under the peak of dodecane used as the external standard; m_{St} is the mass of the dodecane (mg); and m is the sample weight (mg).

Biodiesel quality assessment. Some of the most important physicochemical properties of the biodiesel produced were determined using the standardized methods described by the American Society for Testing and Materials (ASTM D-6751). These physicochemical characteristic includes: (I) ester content using gas chromatography (GC); (II) acid value determined by a volumetric titration; (III) density by a data physics dynamic contact angle tensiometer and (IV) viscosity using an Anton Pear Rheometer model Rheolab QC. Finally, the resulted properties were compared with the biodiesel standards set by the European diesel fuel specifications for diesel engines (EN14214) and ASTM D-6751.

Results and discussion

Catalyst characterization

Thermogravimetric analysis. Thermogravimetric analysis was conducted to study the thermal stability of the catalyst and to determine the appropriate calcination temperature of the 10CsCl/NP catalyst. Fig. 1a and b show TG curves of the 10CsCl/

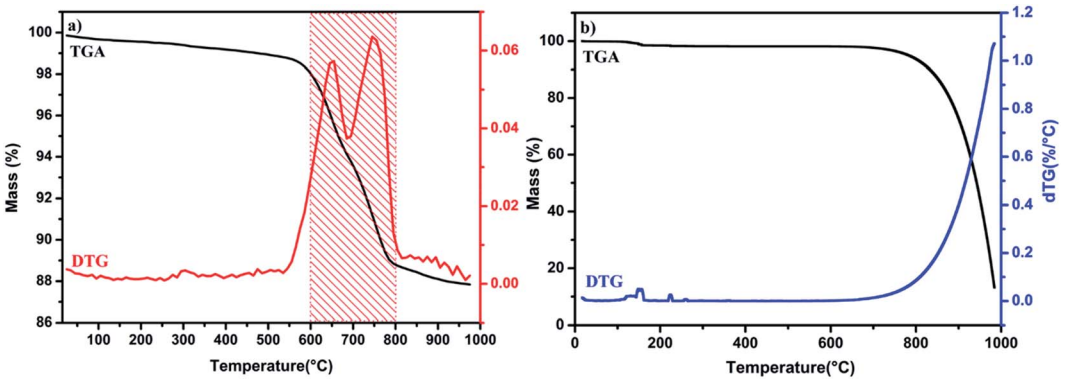

Fig. 1 TGA/DTG curves of (a) 10CsCl/NP and (b) pure CsCl precursor cesium.

PN catalyst and CsCl precursor. As can be seen, the 10CsCl/NP catalyst exhibited generally two weight losses steps between 600 and 780 °C. The first weight loss occurring between 600–700 °C may be due to the thermal decomposition of the CsCl precursor, whereas the second weight loss observed between 700–800 °C could be assigned to the thermal decomposition of the mineral carbonates naturally present in the NP sample.[36,37] The slight weight detected after 800 °C can be indicative of cesium species loss by volatilization phenomenon.[38,39] When comparing the thermal decomposition behavior of pure CsCl alone and when impregnated into NP (TG curve of the 10CsCl/NP), we can clearly observe that the thermal decomposition of the CsCl precursor was significantly accelerated after its impregnation into NP, suggesting that the NP can act as a catalyst for the thermal decomposition of the CsCl precursor. From these observations, to maintain the catalyst stability and to avoid Cs volatilization, the calcination should not exceed 800 °C.

X-ray diffraction. The X-ray diffraction patterns of NP and the conveniently modified natural phosphate are shown in Fig. 2. The XRD pattern of treated NP shows typical diffractions peaks of carbonate-fluoroapatite (JCPDS card 01-073-9695)[33] as the main mineralogical phase in combination with two other secondary phases attributed to calcite (JCPDS card 96-900-1298) and quartz (JCPDS card 96-901-5023). We note that no other phases such as tricalcium phosphate (β-$Ca_3(PO_4)_2$) or dolomite are observed in the XRD spectrum of NP. Upon impregnation with CsCl and drying at 90 °C, the XRD patterns of dried 10CsCl/NP material shows additional peaks related to the presence of the cubic phase of cesium chloride (JCPDS card 96-900-9744), thus indicating that CsCl precursor was not decomposed during impregnation and drying steps. Calcination up to 650 °C seems to be insufficient to totally decompose the cesium chloride and corresponding diffraction peaks still remain in the XRD pattern of samples calcined at a temperature below 650 °C (Fig. 2). Although CsCl peaks disappears in the case of the sample calcined at 800 °C. Fig. 2 shows that only the characteristic peaks of the apatite structure were detected, suggesting that the CsCl precursor was thermally decomposed and that the cesium species were partially incorporated into the apatite structure and regulate its acid–base properties, thus resulting in the generation of different catalytically active sites.[40] Furthermore, the XRD pattern of calcined sample shows the disappearance of diffractions peaks relative to calcite and quartz. This suggests that the quartz (SiO_2) was either transformed into amorphous silica or it was incorporated into the calcium phosphate lattice resulting in a silicon-substituted apatite,[27] whereas the disappearance of the diffraction peaks of the calcite suggests that this phase was totally decomposed during the thermal treatment. As shown in Fig. 2, the obvious peak shift of the most intense

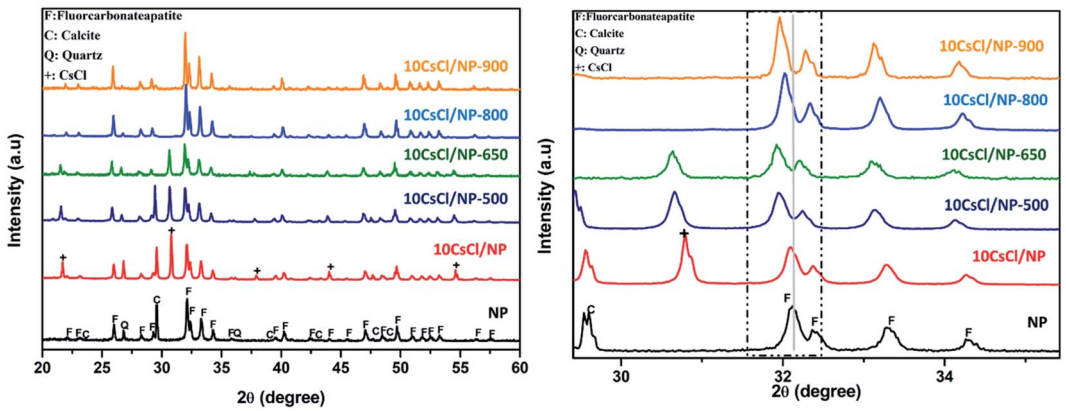

Fig. 2 XRD patterns of natural phosphate, uncalcined 10CsCl/NP and calcined samples.

diffraction peak assigned to the 211 diffraction plan toward lower diffraction angles of the 10CsCl/NP sample calcined at 800 °C compared to unmodified NP implies that Cs species have been partially incorporated into the apatite structure. It should be pointed out that the quantity of cesium possibly incorporated in the apatite structure is not sufficient to generate a visible variation of the lattice parameters as shown in Table 2. However, the incorporation is accompanied by a significant increase in the cell volume due to the difference in ionic radius between cesium ($rCs^{+} = 1.78$ Å) and the calcium ($rCa^{2+} = 1.00$ Å) of the apatite structure.

FTIR spectroscopy. The FTIR spectra of NP and 10CsCl/NP-800 in the range of 400–4000 cm^{-1} are shown in Fig. S1 (ESI†). According to this figure, many characteristic bands of apatite structure have been observed. The bands located at 570 and 606 cm^{-1} could be assigned to antisymmetric deformation (ν_4) of PO_4 group, whereas the band observed at 1045 cm^{-1} could be attributed to the asymmetric stretching vibration (ν_3) of PO_4 group.[41] In addition, the band appearing at 3648 cm^{-1} and those observed at 3440 and 1645 cm^{-1} could be assigned to the stretching mode of hydroxyl OH and the bending/stretching vibrations mode of the physically adsorbed water molecules, respectively.[42] The band located at 1450 cm^{-1} is contributed to the presence of CO_3^{2-} species in sample.[43]

^{31}P NMR MAS of NP and 10CsCl/NP-800. ^{31}P NMR MAS experiments were conducted to investigate the chemical environment around the phosphorus in the prepared catalyst. The ^{31}P magic angle spinning (MAS) solid state NMR spectra of the NP and the conveniently modified 10CsCl/NP-800 are shown in Fig. 3. According to the ^{31}P NMR results it is obvious that the ^{31}P MAS-NMR spectrum of the NP shows the presence of one a single isotropic narrow signal at 4.69 ppm suggesting the presence of one type of phosphorus group (PO_4^{3-}) in the NP sample and that all the phosphorus group are chemically equivalent. Similarly, the conveniently modified 10CsCl/NP-800 exhibited also one single isotropic narrow signal at 4.72 ppm indicating that the sample contains one type of phosphorus group (PO_4^{3-}).[44] Here, we would like to point out that no additional signals attributed to the presence of cesium phosphate or other compound containing phosphorus element were detected, these results were in agreement with those obtained with the XRD results.

Specific surface area, pore diameter and pores volume. Textural properties of the NP and the conveniently modified 10CsCl/NP-800 catalyst specifically the BET surface area, pore diameter and pore volume determined from the nitrogen adsorption/desorption isotherms at 77 K are summarized in Table 3. The BET surface area, average pore diameter and pore volume of NP were 4.93 $m^2\ g^{-1}$, 3.64 nm and 0.01583 $cm^3\ g^{-1}\ nm^{-1}$, respectively. After impregnation and calcination, the BET surface area gradually decreased from 4.93 to 2.85 $m^2\ g^{-1}$ and the average pore diameter determined from nitrogen sorption isotherm analysis significantly decreased from 3.64 to 3.31 nm as the loading level of CsCl was increased from 0 to 10 wt%. The pore volume follows the same behavior and decreased from 0.01583 to 0.00718 $cm^3\ g^{-1}$ upon chemical impregnation and thermal treatment. Such decrease in surface area, pore diameter and pore volume could be ascribed to the fact that the surface and the pores of the catalyst were covered and filled by the Cs species. In addition, the sintering effect of the catalyst particles at high calcination temperature could also leads to the agglomeration of catalyst particle and the collapsing of the pores, thus resulting in a significant decrease of the specific surface area. Similar behavior was also reported in literature when using a preparation method similar to that used in the present work.[23] The data in Table 3 suggests that the transesterification reaction could occurs favorably over the external and internal surface of the catalyst.[45,46] The basic strengths of the NP and 10CsCl/NP 800 were determined by phenol adsorption and the obtained results are listed in Table 3. According to data, the total basicity of the 10CsCl/NP 800 catalyst was significantly increased after impregnation by CsCl and calcination at 800 °C for 4 hours. The total basicity was found to increase from 5.31 to 21 μmol g^{-1} for NP and the 10CsCl/NP 800 catalyst, respectively. This increase in total basicity could be due to the generation of new basic sites resulting upon the incorporation of cesium species inside the apatite structure by the chemical impregnation and calcination processes.

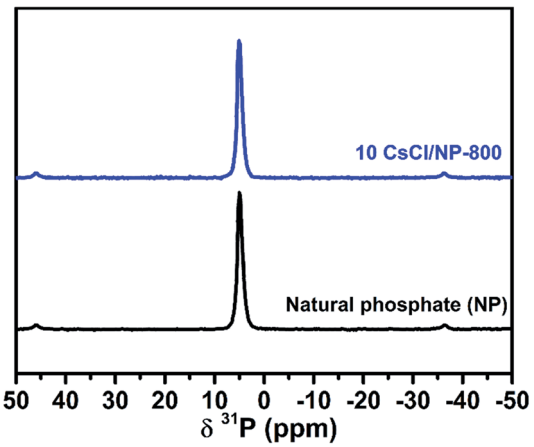

Fig. 3 ^{31}P MAS-NMR spectra of NP and 10CsCl/NP-800.

Table 2 Lattice parameters and cell volume of NP and 10CsCl/NP-800

	Lattice parameters		
Material	$a = b$ (Å)	c (Å)	Volume (Å^3)
NP	9.3256	6.8678	517.2619
10CsCl/NP-800	9.3490	6.8741	520.3380

Scanning electron microscopy. The surface morphology of the NP and the 10CsCl/NP catalyst calcined at 800 °C was observed by SEM. The visual assessment of SEM images in Fig. 4 revealed that there is a significant change in the surface morphology of the NP after chemical impregnation. SEM micrographs of the NP showed that this mineral had a heterogeneous microstructure and is mainly composed of particles of

Table 3 Textural properties and basic strength of the NP and CsCl/NP catalysts

Catalyst	BET specific area ($m^2\ g^{-1}$)	Pores diameter (nm)	Pores volume ($cm^3\ g^{-1}$)	Basicity ($\mu mol\ g^{-1}$)
NP	4.93	3.64	0.01583	5.31
5CsCl/NP-800	3.30	3.53	0.01025	—
10CsCl/NP-800	2.85	3.31	0.00718	21

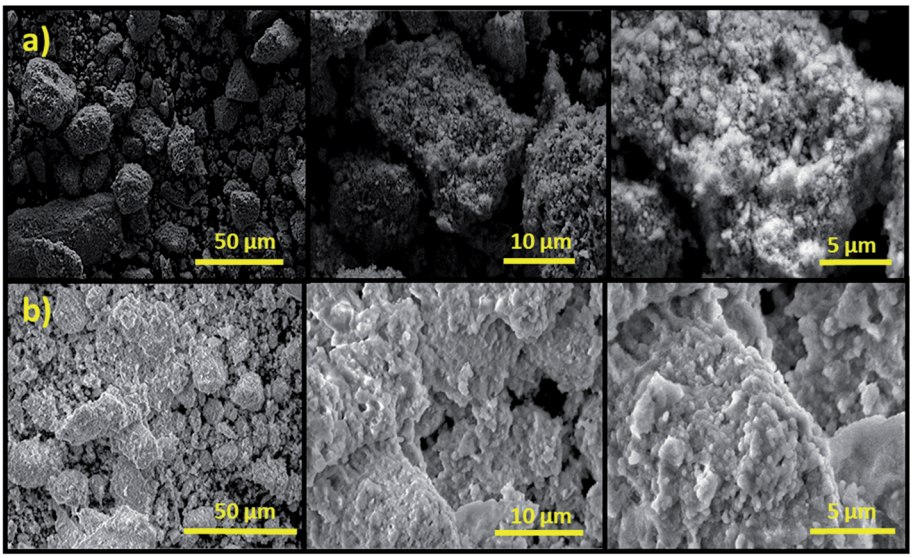

Fig. 4 SEM micrographs of (a) NP and (b) 10CsCl/NP calcined at 800 °C.

irregular geometries in the agglomerated form.[47] SEM images of the 10CsCl/NP-800 illustrate that the surface morphology of the prepared catalyst become more compact and dense in which the catalyst particles adopt a morphology of blocks. Moreover, the catalyst particles tend to agglomerate after being impregnated with CsCl because cesium covers all the pores and surface of the NP, resulting in a very dense and highly agglomerated microstructure.

The elemental analysis by energy dispersive spectroscopy (EDS) of the 10CsCl/NP-800 catalyst was performed in different selected zones during SEM analysis. According to the obtained results, it was clearly observed that 10CsCl/NP-800 is mainly composed of Ca, P, O, C and Cs as major elements in addition to other minor elements like magnesium and silicon, *etc.* From these results, and from the XRD patterns, we suggest that cesium was successfully and regularly distributed over the surface of the catalyst (Fig. 5).

Catalytic activity

Influence of catalyst preparation conditions

Firstly, preliminary experiments were conducted to find out the appropriate catalyst preparation conditions allowing obtaining a maximum rapeseed oil conversion. To do this, a series of CsCl/NP samples with the loading amount of CsCl ranging from 5 to 50 wt% were prepared and their catalytic activity was evaluated in the methanolysis of rapeseed oil under the following reaction conditions: methanol to oil molar ratio of 8 : 1, reaction temperature of 80 °C, catalyst amount of 4 wt% based on oil weight and reaction time of 6 h. The dependence of the catalytic activity of the CsCl/NP catalyst on the impregnation ratio is shown in Table 4. According to data in this table, it is clearly observed that the CsCl precursor was inactive for the transesterification of rapeseed oil with methanol, whereas the unmodified NP was able to catalyze this reaction allowing obtaining a low rapeseed oil conversion of 41%. Upon impregnation with CsCl and calcination, the catalytic activity of the CsCl/NP was found to gradually increase. Indeed, when the loading level of CsCl increased from 5 to 10 wt%, the rapeseed oil conversion was found to increase from 17 to 90.02%. The use of catalysts having a loading level of CsCl up to 50 wt% did not bring an increase in rapeseed oil conversion, hence, the catalyst impregnated with 10 wt% of CsCl and calcined at 800 °C was chosen as the optimal catalyst for the transesterification of the rapeseed oil with methanol.

Influence of reaction conditions

The transesterification process strongly depends on the reaction conditions used such as reaction temperature, methanol to oil molar ratio, catalyst amount and reaction time. In the present work, all these parameters were studied using the pre-

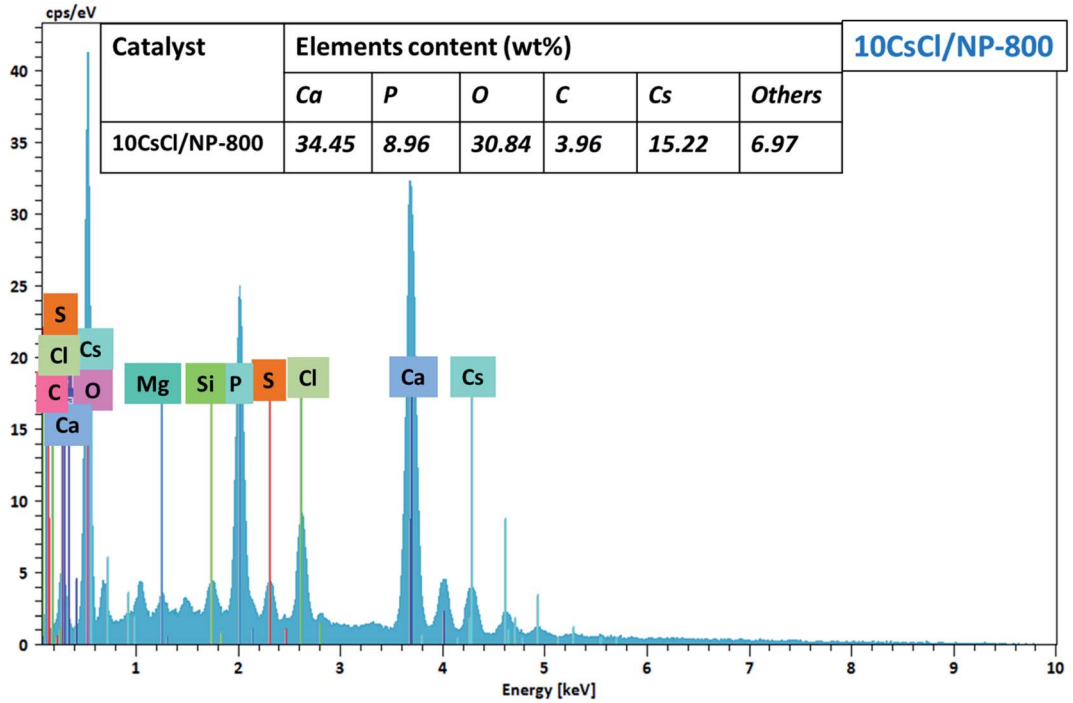

Fig. 5 Semi quantitative EDX analysis of the 10CsCl/NP-800.

Table 4 Catalysts screening and effect of loading level of CsCl on the rapeseed oil conversion

Entry	Catalysts	Loading level of CsCl (%)	Calcination temperature (°C)	Rapeseed oil conversion (%)
1	CsCl	—	—	2
2	NP	—	700	41
3	5CsCl/NP	5	800	17
4	10CsCl/NP	10	800	90.02
5	30CsCl/NP	30	800	89.7
6	50CsCl/NP	50	800	91

optimized 10CsCl/NP-800 in order to find out the optimum reaction parameters for a maximum FAME yield.

The effect of reaction temperature on rapeseed oil conversion was investigated by varying the reaction temperature in the range 40–80 °C as shown in Fig. 6a, while keeping the other experimental constant *i.e.* methanol to oil molar ratio using 8 : 1, catalyst loading of 4 wt% and reaction time of 6 h. By increasing the reaction temperature from 40 to 70 °C, the rapeseed oil conversion was found to increase from 1 to 90.02%. Such increase in oil conversion with the increase in reaction temperature from 40 to 70 °C was expected since higher reaction temperature accelerates the intrinsic rate constant of the transesterification reaction by increasing the collision among the reactants molecules thereby enhances the miscibility and mass transfer.[48] However, further increase in the reaction temperature up to 80 °C did not affect the rapeseed oil conversion significantly. The obtained results showed that the optimum conversion of 90.02% was obtained at a reaction temperature of 70 ± 0.5 °C.

Since the transesterification reaction occurs in an immiscible three-phases system consisting of oil–methanol–catalyst, the progress of the transesterification reaction is significantly affected by the agitation speed which is considered one of the most limiting parameters that affects the reaction progress.[49] In the present study, the agitation speed was kept constant and equal to 800 rpm all through the transesterification experiments in order to avoid its influence on the reaction rate.

To find out the optimal catalyst amount allowing obtaining optimal oil conversion, series of transesterification reactions were conducted by varying the amount of the 10CsCl/NP-800 catalyst from 2 to 8 wt% with respect to initial oil weight. The results obtained clearly indicate (Fig. 6b) that the rapeseed oil conversion increased as the catalyst amount was increased from 2 to 4 wt% and attained an optimum value of 90.02% at 4 wt%. Using higher catalyst loading (6–8 wt%), the FAME yield was not found to change significantly. Therefore, catalyst amount of 4 wt% was chosen as the optimum value. The increase in rapeseed oil conversion with increasing the amount of catalyst could be ascribed to the increase of the number of the available

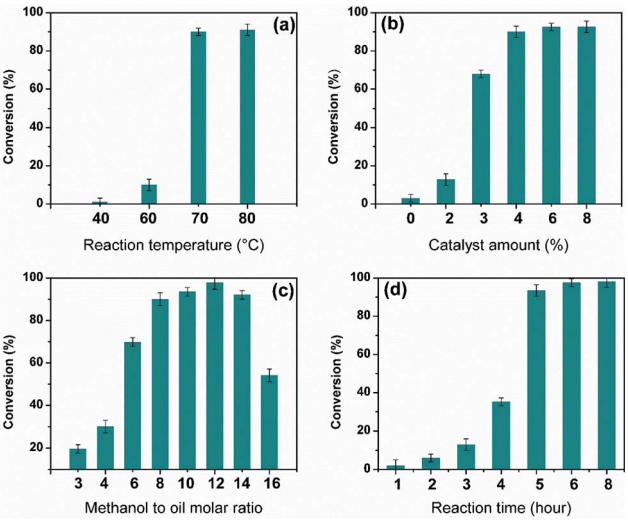

Fig. 6 Influence of reaction conditions on rapeseed oil conversion: (a) effect of reaction temperature, (b) influence of catalyst amount (c) dependence of rapeseed oil conversion on methanol to oil molar ratio and (d) effect of reaction time.

active catalytic sites able to promote the transesterification reaction.[50] However, this correlation is not always linear because at high catalyst concentration the reaction mixture becomes too viscous which can reduce the mass transfer between oil and methanol and thus decrease the biodiesel yield.[51]

The transesterification reaction occurs in three consecutive steps in which the triglyceride molecule is converted into diglyceride molecule which is converted into monoglycerides which is in turn converted into methyl esters along with glycerol as a by-product.[6] Stoichiometrically, the transesterification reaction requires 3 moles of methanol to react with one mole of triglyceride to produce three moles of FAMEs and one mole of glycerol. Since the transesterification reaction is reversible, excess of methanol is usually needed to drive the reaction equilibrium towards FAME formation. Furthermore, excess of methanol is usually used to reduce the viscosity of the reaction medium and eventually to enhance the mass transfer. The effect of methanol to oil molar ratio on rapeseed oil conversion was investigated by performing a series of transesterification experiments by varying the molar ratio from 3 : 1 to 16 : 1, while fixing the other reaction parameters: catalyst amount of 4 wt%, temperature of 70 °C and reaction duration of 6 hours. The results (Fig. 6c) showed that the oil conversion increased with increasing methanol to oil molar ratio up to 12 : 1 and reached a maximum value of 99.55%. Large excess of methanol promote the formation of plenty of methoxy species on the 10CsCl/NP-800 catalyst surface, thus leads the reaction equilibrium towards FAME production thereby, increases the oil conversion.[52] However, further increase in the methanol to oil molar ratio beyond 12 : 1 did not promote the reaction and the oil conversion was found to decrease dramatically. This drop in oil conversion could be due to the ability of glycerol, formed during the reaction, to dissolve in the excess methanol, inhibiting the reaction alcohol with the reactants.[53] Therefore, methanol to oil molar ratio of 12 : 1 was selected as an optimum ratio.

The effect of reaction duration on rapeseed oil conversion was investigated by performing the transesterification experiments at various reaction times ranging from 1 to 8 hours under the following reaction conditions: catalyst amount of 4 wt%, methanol to oil molar ratio of 12 : 1 and reaction temperature of 70 °C. According to Fig. 6d, the rapeseed oil conversion was very low during the first three hours and did not exceed 20%. After extending the reaction time to 6 hours, biodiesel conversion increased and reached a conversion of 99.55%. No significant change was obtained when the duration was extended to 8 hours. Therefore, a duration of 6 hours was selected as the optimal reaction duration for maximum oil conversion.

The progress of rapeseed oil conversion to the corresponding methyl esters over time was monitored by ^{1}H-NMR by collecting the ^{1}H-NMR spectra of reaction products withdrawn at different time intervals. Typical ^{1}H-NMR spectra of samples withdrawn at

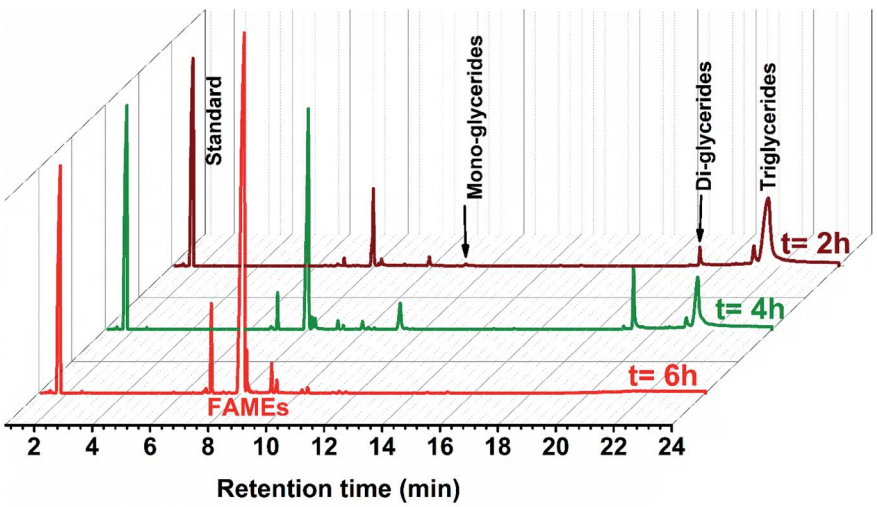

Fig. 7 Evolution of GC chromatograms of biodiesel synthesized from transesterification of rapeseed oil over time.

Table 5 FAMEs, monoglyceride (MG), diglycerides (DG) and triglyceride (TG) contents of the biodiesel

	Biodiesel component				
Products	FAME (%)	MG (%)	DG (%)	TG (%)	FFA (%)
After 2 h	15.68	2.38	3.66	76.08	2.17
After 6 h	99.55	0.18	0.26	—	—

Table 6 Acid values of oleic acid/rapeseed oil mixture before and after reaction

		Acid value (mg_{KOH} g^{-1})		
Entry	Oleic acid content (wt% of oil)	Before reaction	After reaction	Conversion (%)
1	0.5	2.31	0.62	73.16
2	1	3.92	1.2	69.38
3	2.5	8.69	2.88	66.85
4	5	13.35	8.39	37.15

different time intervals are shown in Fig. S2 (ESI†). According to this figure, as the reaction progress, the intensity of the signals associated with protons attached to the glyceryl methine (–CH–O) observed at 5.27 ppm and those of triacylglycerols ($–CH_2–O–$) observed at 4.10–4.33 ppm was found to decrease.[35] For sample withdrawn at reaction times below 4 hours, the presence of those signals indicates that the mixture contains mono, di and triglycerides moieties, pointing to an incomplete transesterification transformation.[34] For a duration above 4 hours, the disappearance of those signals is accompanied with the appearance of a new strong singlet located at 3.67 ppm assigned to the protons of methoxy group of methyl esters signal.[34] In the ^{1}H-NMR spectra of the reaction product withdrawn at 6 hours, the above mentioned signals were clearly missing, suggesting a complete conversion of rapeseed oil into the corresponding methyl esters.

The FAME, monoglyceride (MG), diglycerides (DG) and triglyceride (TG) contents were determined by GC using dodecane as internal standard. Fig. 7 show the GC chromatograms of the obtained products at various interval times (2, 4 and 6 hours) and Table 5 show FAMEs, MG, DG and TG contents of samples collected after 2 and 6 hours of reaction, respectively.

Within the first 2 hours of reaction, the resulting product contains 15.68 wt% of FAMEs, 2.38 wt% of MG, 3.66 wt% of DG and 76.08 wt% of TG. After reaction completion, the MG and DG contents were around 0.18 and 0.26 wt%, respectively, whereas the ester content was found to reach 99.55 wt%.

On the basis of the above-mentioned optimization results, the following reaction conditions: methanol to oil molar ratio of 12 : 1, reaction temperature of 70 °C, catalyst amount of 4 wt%, reaction time of 6 h and 800 rpm agitation speed have been selected as the optimal parameters for rapeseed oil transesterification by methanol over 10CsCl/NP-800 catalyst. To the best of our knowledge, this is the first report, which states the successful utilization of cesium modified natural phosphate as a catalyst for biodiesel production.

Esterification/transesterification of acidified rapeseed oil

Low grade oil feedstocks such as crude vegetable oils, waste cooking oils and animal fats contain usually high content of free fatty acids which leads to side reactions *i.e.* soap formation during the base-catalyzed transesterification.[53] Additionally, it was reported that the base-catalyzed transesterification cannot tolerate feedstocks having an acid value higher than 2 mg_{KOH} g^{-1}.[54] The purpose of the present study was done to determine whether our catalyst is able to perform esterification and transesterification reactions simultaneously so that FFA present in the acidic oil can be converted into FAME. In the present work, acidified oils were prepared by mixing different amounts of oleic acid (0.5 to 5 wt% based on oil weight) with rapeseed oil to simulate models of low-grade acidic oils. The acid value of the resulting mixture was determined by titrimetric method according to the method reported in the literature.[55] The esterification experiments were performed under the optimal reaction conditions obtained in this work and the results are listed in Table 6. Data in this table showed that the acid values of the starting oils were significantly reduced after reaction completion. Data in Table 6 showed that the oleic acid conversion reached 73.16, 69.38, 66.85 and 37.15% for oils having an oleic acid content of 0.5, 1.0, 2.5 and 5.0 wt%, respectively. This signifies that our catalyst exhibits good catalytic activity toward the esterification of free fatty acids in a fatty acid/triglyceride mixture. For example, our catalytic system exhibited a good tolerance towards FFA up to 1 wt% (*i.e.* 3.92 mg_{KOH} g^{-1}) and it can reduce the acid value to 1.2 mg_{KOH} g^{-1}. However, further increase in the oleic acid contents in the initial feedstock cause higher acid value final products. Herein, we have remarked that our catalytic system was not efficient to promote the transesterification of rapeseed oil since a low triglyceride conversion, which not exceed 8%, was reached. The obtained results indicate that in our conditions the esterification and transesterification reactions cannot occur simultaneously.

In an attempt to enhance the FAME yield, the organic phase resulting from the experiment conducted according to the entry 2 (Table 6) containing esterified and non-esterified FFA, untransesterified monoglycerides, diglycerides and triglycerides was introduced in a second batch reaction as a raw feedstock. The reaction mixture was first centrifuged to remove the catalyst and then a freshly prepared catalyst was added to the mixture and the reaction mixture was allowed to react for six additional hours without methanol addition. After reaction completion, the catalyst was separated, and the excess methanol was removed under reduced pressure. Phase separation of the reaction mixture resulted in the FAME as the upper phase and glycerol as the lower one. The separated methyl esters phase was evaporated under reduced pressure and then analyzed by ^{1}H-NMR. The obtained results indicate that an oil

Table 7 FFA and rapeseed oil conversions before and after two batch transesterification process

	1st batch reaction		2nd batch reaction	
Initial acid value (mg_{KOH} g^{-1})	A.V (mg_{KOH} g^{-1})	Oil conversion (%)	A.V (mg_{KOH} g^{-1})	Oil conversion (%)
3.92 mg_{KOH} g^{-1}	1.2	8	0.44	93

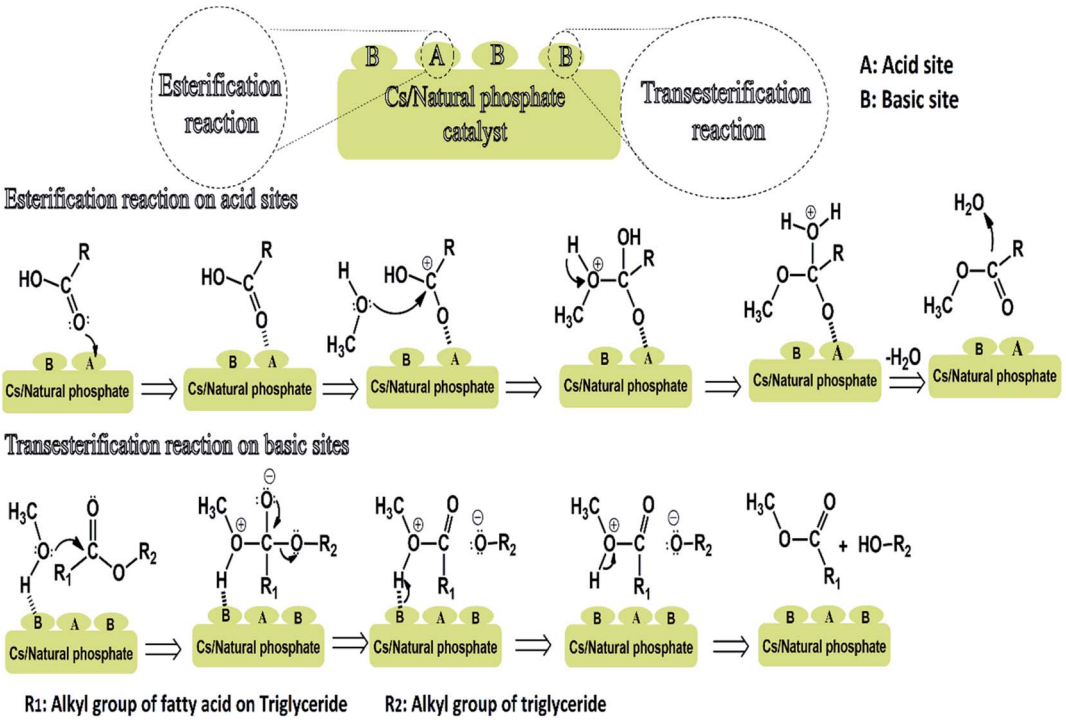

Scheme 1 Plausible esterification/transesterification reaction mechanism over 10CsCl/NP-800.

conversion of about 93% was reached after the second batch reaction (Table 7). Interestingly, the acid value of the produced biodiesel was reduced from 1.2 to 0.44 mg_{KOH} g^{-1} (Table 7), suggesting that both transesterification and esterification reactions occurred simultaneously during the second batch reaction.

Waste cooking oil transesterification

Biodiesel production from feedstocks not competing with food industry, such as waste cooking oil (WCO), animal fats, and crude vegetable oils is considered a cost-effective and economic alternative approach.[56,57] In the present work, the catalytic performance of the 10CsCl/NP-800 catalyst was evaluated in the transesterification of low FFA WCO. Results from GC revealed that a FAMEs yield of 99.52% was achieved in one step transesterification reaction. More interestingly, the acid value of the resulting biodiesel was significantly decreased from 1.06 mg_{KOH} g^{-1} to 0.45 mg_{KOH} g^{-1}. This result definitely indicates that our developed catalyst is efficient in catalyzing the transesterification of low free fatty acid oils, thus giving rise to a potentially applicable catalyst for second generation biodiesel production.

Possible reaction mechanism using 10CsCl/NP-800 catalyst

The NP is quite complex material due to its large versatility of composition. It contains both Lewis and Brønsted basic sites which serve as active catalytic sites for many chemical reactions. The existence of surface OH, Ca^{2+}–OH^{-}, POH–OH and O_2^{-} on the surface of the NP framework indicates that both basic and

Table 8 FAMEs profile of the rapeseed oil and WCO biodiesel

		Composition of biodiesel	
Methyl ester	FAME structure	RO (%)	WCO (%)
Methyl palmitoleate	C16:1	0.59	0.25
Methyl palmitate	C16:0	6.45	13.14
Methyl linoleate	C18:2	16.98	56.98
Methyl oleate	C18:1	69.45	21.74
Methyl stearate	C18:0	2.76	5.59
Methyl eicosanoate	C20:1	2.04	0.80
Methyl arachidate	C20:0	0.97	0.79
Others	—	0.72	0.67

Table 9 Physicochemical properties of the biodiesel prepared by transesterification of rapeseed oil and waste cooking oil

Property	Biodiesel from RO	Biodiesel from WCO	Norme EN14214	Norme ASTM D6751
Ester content % (m m^{-1})	99.55	99.52	96.5 min	96.5 min
Monoglycerides	0.18	0.47	0.70 max	0.4 max
Diglycerides	0.26	—	—	—
Acid number (mg_{KOH} g^{-1})	0.35	0.45	0.5 max	0.5 max
Density (kg m^{-3})	875	893	860–900	—
Kinematic viscosity at 40 °C (mm^2 s^{-1})	4.34	4.94	3.5–5	1.9–6.0

acidic sites are present on catalyst surface. The presence of numerous isomorphic substitutions (Ca by Mg and PO_4^{3-} by CO_3^{2-}) can also reinforces the catalytic activity and bring about new active catalytic sites. This explain why NP alone have a moderate catalytic activity. Moreover, the impregnation of cesium species in the NP framework can also reinforces the catalytic activity of our catalyst by generating new active catalytic sites. We believe that both acid and basic sites on its surface are involved in the reaction mechanism. The presence of the Lewis acidic sites promote the fatty acid esterification and leads to the reduction of the acidity of the feedstock and the existence of basic sites could promote the transesterification reaction of triglyceride moieties to yield fatty acid methyl esters or biodiesel. For the esterification reaction, FFAs were first adsorbed on catalyst surface catalyst, then the interaction between the carbonyl oxygen of the FFA and the Lewis acidic site of the catalyst (A) led to generation of carbocation (electrodeficient carbon) (Scheme 1). Nucleophilic attack by the methanol's oxygen atom present in the reaction mixture on the generated carbocation led to the formation of a tetrahedral intermediate. Subsequently, an internal rearrangement followed by the elimination of water molecule from the intermediate resulted in the production of methyl oleate.

In transesterification reaction, the reaction mechanism involves the similar mechanism as esterification reaction but after the elimination of esters molecule, the reaction extends to di- and monoglycerides. Basically, the catalytic basic sites (B) activate methanol through interactions with the proton of the OH group of methanol molecule and generates a reactive nucleophile. Subsequently, the triglyceride moiety adsorbed on the surface of the catalyst interacts with the active nucleophile *via* the carbonyl group and led to the formation of an intermediate. Further, an internal rearrangement led to the formation of one mole of fatty acid methyl ester and diglyceride as a by-product. The formed diglyceride reacts with adsorbed methanol to yield one mole of fatty acid methyl ester and monoglyceride as a by-product. In his turn, monoglyceride react with active nucleophile to yield one mole of fatty acid methyl ester and glycerol as a by-product.

Biodiesel characterization

Biodiesels produced from rapeseed oil and low FFA waste cooking oil under optimal conditions were analyzed using GC-MS in scan mode to identify the FAMEs profiles using NIST 2011 MS Library. Typical GC chromatograms of the 1st and 2nd generation biodiesel are shown in Fig. S3 (ESI†) and Fig. S4 (ESI†), respectively. The different peaks reveal the presence of various methyl esters. FAMEs profiles are given in Table 8. The intense peaks indicate the presence of methyl oleate and methyl linoleate as major components in both RO and WCO biodiesels. Some important physical and chemical properties of the obtained biodiesels prepared from rapeseed and WCO feedstocks are listed in Table 9. The results showed that the major properties of the produced biodiesel fulfil the requirements specified by EN14214 and the ASTM D6751 standards for biodiesel. The ester content, expressed as weight percentage, of the produced biodiesel was found to be higher than the limit value 96.5%. The MG and DG contents were below the limit values specified by the EN14214 standard. Herein, the waste cooking oil biodiesel showed higher viscosity compared to the rapeseed oil biodiesel. This could be due to the difference in FAMEs composition between the two products.[58]

Conclusion

The cesium modified natural phosphate prepared by chemical impregnation of NP by cesium chloride was successfully used for biodiesel production from low FFA feedstocks. The impregnation of NP by cesium resulted in the incorporation of cesium species in the apatite lattice, thus leading to generation of numerous actives sites on the catalyst. The catalyst impregnated by 10 wt% of CsCl and calcined at 800 °C for 4 h was determined to be the best catalyst among the studied catalysts. The transesterification reaction was suggested to occur over the internal and external surface of the 10CsCl/NP-800 °C catalyst since the transesterification rate was not found to be dependent on the catalyst surface area. The determination of basicity indicated that the 10CsCl/NP-800 catalyst has a predominantly strong basic sites compared to NP. The catalytic activity of the 10CsCl/NP-800 catalyst for the transesterification rapeseed oil was found to be related to the density and strength of acid–basic sites. Maximum biodiesel yield in terms of ester content was found to reach 99.55% under the following optimized conditions: methanol to oil molar ratio of 12 : 1, reaction temperature of 70 °C, catalyst amount of 4 wt%, reaction time of 6 h and 800 rpm agitation speed. The 10CsCl/NP-800 catalyst was also demonstrated to be active to the esterification of oleic acid added to rapeseed oil and was able to reduce the acidity of the acidified feedstocks. The 10CsCl/NP-800 catalyst showed

tremendous potential in biodiesel production from waste cooking oil.

Conflicts of interest

The authors declare that they have no competing interests.

Acknowledgements

The assistance of the University Hassan II Casablanca and MAScIR Foundation, towards this research is hereby acknowledged. The authors also express their gratitude for the financial assistance provided by the Delegate Ministry for the Environment through the MDE's Environmental R&D Support Program.

References

1 E. M. Shahid and Y. Jamal, *Renewable Sustainable Energy Rev.*, 2011, **15**, 4732–4745.
2 S. H. Teo, A. Islam and Y. H. Taufiq-Yap, *Chem. Eng. Res. Des.*, 2016, **111**, 362–370.
3 C. C. A. Loures, M. S. Amaral, P. C. M. Da Rós, S. M. F. E. Zorn, H. F. De Castro and M. B. Silva, *Fuel*, 2018, **211**, 261–268.
4 J. M. Dias, M. C. M. Alvim-Ferraz and M. F. Almeida, *Fuel*, 2008, **87**, 3572–3578.
5 A. Martínez, G. E. Mijangos, I. C. Romero-Ibarra, R. Hernández-Altamirano and V. Y. Mena-Cervantes, *Fuel*, 2019, **235**, 277–287.
6 S. Zhang, Y. Zu, Y. Fu, M. Luo, D. Zhang and T. Efferth, *Bioresour. Technol.*, 2010, **101**, 931–936.
7 M. E. Borges and L. Díaz, *Renewable Sustainable Energy Rev.*, 2012, **16**, 2839–2849.
8 I. M. Atadashi, M. K. Aroua, A. R. A. Aziz and N. M. N. Sulaiman, *J. Ind. Eng. Chem.*, 2013, **19**, 14–26.
9 C. S. Macleod, A. P. Harvey, A. F. Lee and K. Wilson, *Chem. Eng. J.*, 2008, **135**, 63–70.
10 R. S. Watkins, A. F. Lee and K. Wilson, *Green Chem.*, 2004, **6**, 335–340.
11 A. Z. Abdullah, N. Razali and K. T. Lee, *Fuel Process. Technol.*, 2009, **90**, 958–964.
12 M. Farooq, A. Ramli, A. Naeem and M. Saleem Khan, *RSC Adv.*, 2016, **6**, 872–881.
13 N. Pasupulety, K. Gunda, Y. Liu, G. L. Rempel and F. T. T. Ng, *Appl. Catal., A*, 2013, **452**, 189–202.
14 V. Mahdavi and A. Monajemi, *J. Taiwan Inst. Chem. Eng.*, 2014, **45**, 2286–2292.
15 Y. Wang, H. Chou, B. Chen and D. Lee, *Bioresour. Technol.*, 2013, **145**, 248–253.
16 C. Liu, W. Lu and T. Liu, *Energy Fuels*, 2012, **26**, 5400–5407.
17 H. Amani, M. Asif and B. H. Hameed, *J. Taiwan Inst. Chem. Eng.*, 2016, **58**, 226–234.
18 M. Verziu, M. Florea, S. Simon, V. Simon, P. Filip, V. I. Parvulescu and C. Hardacre, *J. Catal.*, 2009, **263**, 56–66.
19 J. Nisar, R. Razaq, M. Farooq, M. Iqbal, R. Ali, M. Sayed and A. Shah, *Renewable Energy*, 2017, **101**, 111–119.
20 R. Ghanei, R. K. Dermani, Y. Salehi and M. Mohammadi, *Waste Biomass Valorization*, 2016, **7**, 527–532.
21 G. Chen, R. Shan, J. Shi, C. Liu and B. Yan, *Energy Convers. Manage.*, 2015, **98**, 463–469.
22 R. Chakraborty and D. Roychowdhury, *J. Taiwan Inst. Chem. Eng.*, 2013, **45**, 92–100.
23 Y. Essamlali, O. Amadine, M. Larzek, C. Len and M. Zahouily, *Energy Convers. Manage.*, 2017, **149**, 355–367.
24 Y. Essamlali, O. Amadine, A. Fihri and M. Zahouily, *Renewable Energy*, 2018, **133**, 1295–1307.
25 F. Bazi, H. El Badaoui, S. Tamani, S. Sokori, L. Oubella, M. Hamza, S. Boulaajaj and S. Sebti, *J. Mol. Catal. A: Chem.*, 2006, **256**, 43–47.
26 M. Zahouily, B. Bahlaouan, S. Abderahim, O. Mohamed and S. Saïd, *React. Kinet. Catal. Lett.*, 2003, **78**, 129–133.
27 S. El Asri, A. Laghzizil, A. Alaoui, A. Saoiabi, R. M. Hamdi, K. El Abbassi and A. Hakam, *J. Therm. Anal. Calorim.*, 2009, **95**, 15–19.
28 S. Sebti, A. Solhy, R. Tahir, S. Abdelatif, S. Boulaajaj, J. A. Mayoral, J. I. García, J. M. Fraile, A. Kossir and H. Oumimoun, *J. Catal.*, 2003, **213**, 1–6.
29 M. Zahouily, B. Bahlaouan, M. Aadil, A. Rayadh and S. Sebti, *Org. Process Res. Dev.*, 2004, **8**, 275–278.
30 D. J. Macquarrie, R. Nazih and S. Sebti, *Green Chem.*, 2002, **4**, 56–59.
31 S. Sebti, A. Solhy, A. Smahi, A. Kossir and H. Oumimoun, *Catal. Commun.*, 2002, **3**, 335–339.
32 A. Hassine, S. Sebti, A. Solhy, M. Zahouily, C. Len, M. N. Hedhili and A. Fihri, *Appl. Catal., A*, 2013, **450**, 13–18.
33 Y. Essamlali, M. Larzek, B. Essaid and M. Zahouily, *Ind. Eng. Chem. Res.*, 2017, **56**, 5821–5832.
34 G. Gelbard, O. Br, R. M. Vargas, F. Vielfaure and U. E. Schuchardt, *J. Am. Oil Chem. Soc.*, 1995, **72**, 1239–1241.
35 L. A. Anderson and A. K. Franz, *Energy Fuels*, 2012, **26**, 6404–6410.
36 A. Aouad, M. Benchanâa, A. Mokhlisse and A. Ounas, *J. Therm. Anal. Calorim.*, 2004, **75**, 887–900.
37 K. Tõnsuaadu, K. A. Gross, L. Plūduma and M. Veiderma, *J. Therm. Anal. Calorim.*, 2012, **110**, 647–659.
38 D. Pletser, T. Ohashi, Y. Yoshii and W. E. Lee, *Prog. Nucl. Energy*, 2018, **109**, 214–222.
39 G. Zhang, Z. Peng and C. Li, *J. Therm. Anal. Calorim.*, 2016, **124**, 1063–1070.
40 X. Li, L. Sun, W. Zou, P. Cao, Z. Chen, C. Tang and L. Dong, *ChemCatChem*, 2017, **9**, 4621–4627.
41 J. Klinkaewnarong, E. Swatsitang, C. Masingboon, S. Seraphin and S. Maensiri, *Curr. Appl. Phys.*, 2010, **10**, 521–525.
42 T. Long, Y.-P. Guo, Y.-Z. Liu and Z.-A. Zhu, *RSC Adv.*, 2013, **3**, 24169–24176.
43 C. C. Silva, H. H. B. Rocha, F. N. A. Freire, M. R. P. Santos, K. D. A. Saboia and A. S. B. Sombra, *Mater. Chem. Phys.*, 2005, **92**, 260–268.
44 J. F. Cawthray, A. L. Creagh, C. A. Haynes and C. Orvig, *Inorg. Chem.*, 2015, **54**, 1440–1445.
45 N. Boz, N. Degirmenbasi and D. M. Kalyon, *Appl. Catal., B*, 2013, **138–139**, 236–242.

46 A. F. Lee, J. A. Bennett, J. C. Manayil, K. Wilson and A. F. Lee, *Chem. Soc. Rev.*, 2014, **43**, 7887–7916.
47 A. S. Hammood, S. S. Hassan, T. A. Mohammed and H. L. Jaber, *SN Appl. Sci.*, 2019, **1**, 436–448.
48 X. Liu, X. Piao, Y. Wang, S. Zhu and H. He, *Fuel*, 2008, **87**, 1076–1082.
49 A. P. Vyas, N. Subrahmanyam and P. A. Patel, *Fuel*, 2009, **88**, 625–628.
50 V. Mutreja, S. Singh and A. Ali, *Renewable Energy*, 2014, **62**, 226–233.
51 B. Gurunathan and A. Ravi, *Bioresour. Technol.*, 2015, **190**, 424–428.
52 S. Soltani, U. Rashid, R. Yunus and Y. H. Taufiq-Yap, *Fuel*, 2016, **178**, 1–10.
53 M. Hsiao, C. Lin and Y. Chang, *Fuel*, 2011, **90**, 1963–1967.
54 R. Sheikh, M. Choi, J. Im and Y. Park, *J. Ind. Eng. Chem.*, 2013, **19**, 1413–1419.
55 G. Knothe, J. Krahl and J. Van Gerpen, *The Biodiesel Handbook*, Elsevier Inc., 2010.
56 M. M. K. Bhuiya, M. G. Rasul, M. M. K. Khan, N. Ashwath and A. K. Azad, *Renewable Sustainable Energy Rev.*, 2016, **55**, 1109–1128.
57 T. M. Yunus, A. E. Atabani, I. Anjum, A. Badarudin, M. S. Khayoon and S. Triwahyono, *Renewable Sustainable Energy Rev.*, 2014, **37**, 840–851.
58 Y. Ali, M. A. Hanna and S. L. Cuppett, *J. Am. Oil Chem. Soc.*, 1995, **72**, 1557–1564.